ACS APPLIED MATERIALS & INTERFACES

Research Article

www.acsami.org

Transfer Printing of Self-Folding Polymer–Metal Bilayer Particles

Al de Leon,[†] Andrew C. Barnes,[‡] Patrick Thomas,[†] Johnathan O'Donnell,[†] Christian A. Zorman,[‡] and Rigoberto C. Advincula*[,†]

[†]Department of Macromolecular Science and Engineering, and [‡]Department of Electrical Engineering and Computer Science, Case Western Reserve University, Cleveland, Ohio 44106, United States

Supporting Information

ABSTRACT: A simple and robust alternative for fabricating stimuli-responsive 2D self-folding films was introduced. The approach combines metal-sputtering, layer-by-layer assembly of polyelectrolytes, and transfer-printing of the bilayer film onto a substrate coated with a sacrificial layer. With this technique, self-folding bilayer films can be fabricated without using harsh chemical etchants, complicated chemical synthesis, or complex lithographic techniques. Upon release, the microsized 2D film is shown to reconfigure into a 3D structure caused by a mismatch in the properties of the individual layers. The actuation of the bilayer film can be triggered by partial swelling due to absorption of water or by partial expansion of one of the layers due to an increase in temperature.

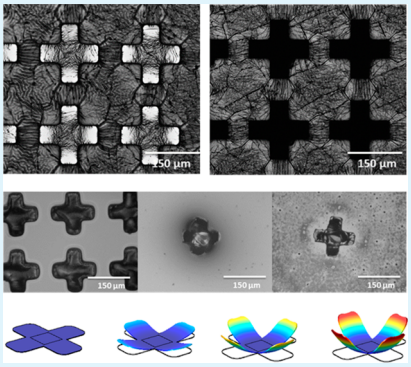

KEYWORDS: *self-folding, transfer printing, stimuli-responsive, polymer–metal bilayer, microcontact printing, FT-IR imaging*

INTRODUCTION

Self-folding films are bilayer systems that spontaneously convert from being 2D to 3D structures upon the application of a stimulus. Stimuli such as temperature, solvent, light, electrical field, capillary forces, and stress-release have been used to actuate the bilayer system.[1−6] Such systems have potential applications as sensors, actuators, and other micromechanical devices.[7,8] It was also demonstrated that self-folding films can be used to encapsulate cells, provide a drug delivery platform, act as a smart wound plaster, and, just recently, act as an untethered tool for microbiopsy.[1,9−12]

Self-folding films are normally composed of at least two parts—an active and a passive layer. The active layer responds to stimulus by either swelling or contracting. Conversely, the passive layer remains unaffected by the applied stimulus and provides the structural rigidity for the whole system. The successful design of self-folding systems requires consideration of the Young's modulus of both the active and the passive layers, the relative and the absolute thicknesses of each layer, and the actuation strain as correlated by the Timoshenko equation.[13] Several self-folding systems have been studied ranging from pure polymeric systems to pure inorganic systems to polymer–inorganic hybrid systems. Ionov et al., for example, fabricated a self-folding pure polymeric system comprising poly(caprolactone) and poly(*N*-isopropylacrylamide) bilayers. They utilized the temperature responsiveness of the poly(*N*-isopropylacrylamide) to encapsulate and release the yeast cells as the 2D film reconfigures into a 3D structure.[1] Gracias et al. used the purely metallic bilayer film composed of differentially stressed chromium and copper layers to reversibly actuate as the copper was oxidized or reduced.[14] Additionally, Huck et al. fabricated a polymer–inorganic self-folding film by combining microcontact printing of the initiator on a gold-coated substrate, surface-initiated polymerization, and etching of the exposed gold substrate. The fabricated gold-cross-linked polymer brush system was shown to respond to solvent by the selective swelling of the polymer layer.[2]

Fabrication of the aforementioned self-folding systems involves either the use of harsh chemical etchants, complicated chemical synthesis, or complex lithographic techniques. Here, a simple and efficient alternative involving the use of the transfer (or microcontact) printing technique was reported. The transfer printing technique has been employed to pattern materials by first depositing them on an elastomeric stamp (usually PDMS). The stamp with the materials is then made in contact on a substrate where the material will stick and be transferred when the elastomeric stamp is removed. There are several microcontact printing techniques, such as multilayer transfer printing and metal transfer printing, but they all share a similar basis. The major difference between techniques is the "ink" they utilize. Multilayer transfer printing uses layer-by-layer assembled polyelectrolytes and metal transfer printing uses thin metal films.[15,16] Multilayer transfer printing involves the alternating adsorption of oppositely charged materials onto the surface of the PDMS stamp. The receiving substrate has a charge opposite to the charge of the top surface of the multilayer film to ensure that it transfers upon contact. It has been used to fabricate (1) sensors from multiwalled carbon

Received: October 3, 2014
Accepted: November 20, 2014
Published: November 20, 2014

Scheme 1. Fabrication of the Self-Folding Polymer–Metal Bilayer

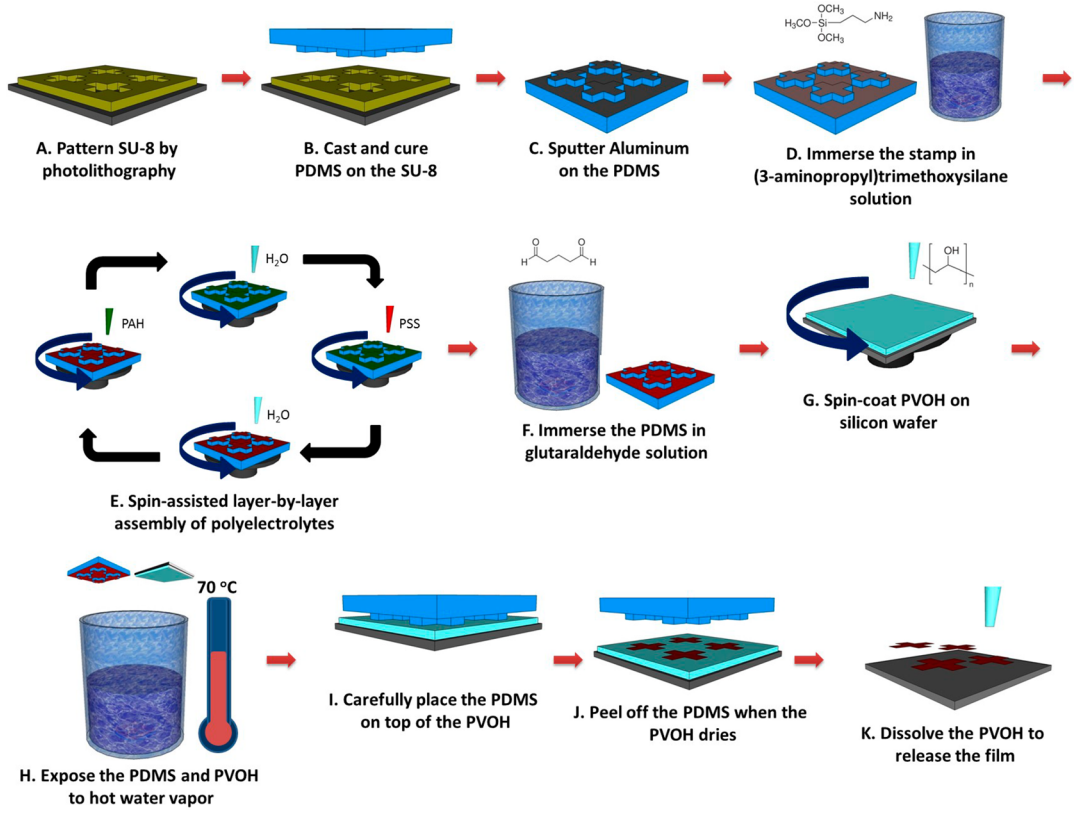

nanotubes, (2) multilayered microparticles, and (3) composite mold for selective immobilization of biomolecules.[17−19] Metal transfer printing, on the other hand, involves the evaporation or sputtering of thin metal film on the PDMS stamp. The patterned metal is transferred by placing the stamp on a polymer-coated substrate (PMMA or PS on silicon wafer) and heating it up above the glass transition temperature of the polymer. This technique has been used to fabricate organic field-effect transistors and other plastic electronics.[20]

In this article, the multilayer transfer technique and the metal transfer technique were combined to fabricate the self-folding bilayer film. The passive layer is a thin aluminum film sputtered directly on the PDMS stamp. The active layer is a multilayered film fabricated by alternating deposition of positively and negatively charged polyelectrolytes, which were then cross-linked. Actuation of the polymer–metal bilayer system is triggered by adding solvent, which swells the polymer layer, or by increasing the temperature, which selectively expands the aluminum layer. This technique shares several advantages with the other microcontact printing techniques: (1) the procedure is simple and easy, (2) it requires minimal use of a cleanroom, (3) multiple stamps can be created from a single master, and (4) individual stamps can be used more than once with minimal degradation of performance.[21]

RESULTS AND DISCUSSION

Fabrication of the self-folding polymer–metal bilayer film is shown in Scheme 1. Thick SU-8 photoresist (10 μm thick), which was patterned using the traditional photolithography procedure, served as the master template for the fabrication of the elastomeric stamp. The mixture of the poly(dimethylsiloxane) (PDMS) base and curing agent (10:1 ratio) was cast on the patterned SU-8 photoresist and cured at 60 °C for 2 h. The cured PDMS (or the PDMS stamp) was carefully peeled off from the master template. Aluminum (100 nm thick) was then sputtered on the PDMS stamp. Silane-based adhesion promoter was self-assembled on the aluminum surface by immersing the aluminum-coated PDMS stamp in 0.5 wt % (3-aminopropyl)trimethoxysilane (APS) solution for 1 h. Positively and negatively charged polyelectrolytes were deposited via spin-assisted layer-by-layer assembly. This enabled fast, efficient, and thickness-controlled fabrication of the polymer swelling layer. One milligram/milliter of poly(allylamine hydrochloride) (PAH) and 1 mg/mL of poly(styrenesulfonate) (PSS) in 0.1 M NaCl were used. The pH of the PAH solution was adjusted to pH = 6.5 to make sure that the PAH was more than 50% ionized (pK_a of PAH = 8–9). Each was deposited in succession with each pair forming a bilayer; several thicknesses with 5, 10, and 15 bilayers of polyelectrolytes were tested, but only the 15 bilayers were observed to respond visibly to solvent and temperature. Thus, the following discussion is more focused on the fabrication and behavior of the polymer–metal system with 15 bilayers of polyelectrolytes. To ensure that the polyelectrolyte remains robust upon the application of the stimuli, the PAH layers were cross-linked by glutaraldehyde. Glutaraldehyde is known to react with the amine-functional group of PAH to form an amide.[22] The PDMS stamp with the film was immersed in 10 wt % glutaraldehyde in water for 2 h. The film was then washed with ample amount of water to remove the unreacted glutaraldehyde. The self-folding film was then transfer-printed to the poly(vinyl alcohol) (PVOH)-coated silicon wafer. The transfer printing was done by first exposing the PDMS stamp with the self-folding film and the PVOH-coated silicon wafer to

70 °C water vapor for about 30 s. Exposure to hot water vapor ensures strong interaction between the multilayered film and the receiving substrate upon contact.[15] The stamp was then carefully placed on top of the PVOH-coated silicon wafer. Slight pressure was exerted to ensure optimal contact between the stamp and the PVOH. After the PVOH sacrificial film was dried, the stamp was slowly peeled off leaving behind the polymer−metal self-folding film. The polymer−metal self-folding film was released from the substrate by dissolving the PVOH by water.

PVOH was chosen as the sacrificial layer because it interacts strongly with the piranha-cleaned silicon wafer (terminated by Si−OH) and the active layer because of hydrogen bonding.[23] If the interaction between the sacrificial layer and the substrate is too weak, then the sacrificial layer will be peeled off the substrate during the transfer-printing. In addition, the self-folding film will not be transferred if the interaction between the sacrificial layer and the active layer is weaker than the interaction between the aluminum and the PDMS stamp.

Figure 1a shows the scanning electron microscope (SEM) image of the PDMS stamp after sputtering the 100 nm thick

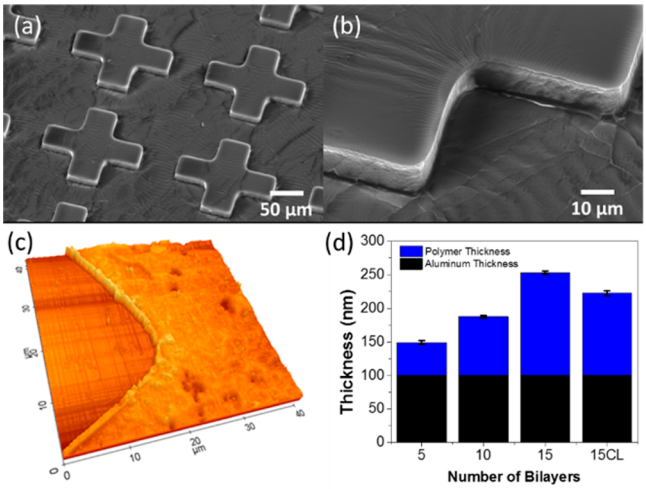

Figure 1. (a, b) Low- and high-magnification SEM images of the PDMS stamp coated with 100 nm aluminum film. (c) AFM topography image of the transfer-printed self-folding film. (d) Thickness of the self-folding film vs the number of bilayers of the polyelectrolytes as measured by AFM.

aluminum film. A close-up look at the edge of the elevated part of the stamp shows that the top and the base were covered with aluminum, but the side was barely coated (see Figure 1b). The discontinuity between the raised regions and the base, and the fact that the adhesion between the aluminum and the PDMS stamp is relatively weak, enabled the efficient transfer-printing of the self-folding film.[24] Figure 1c shows the atomic force microscopy (AFM) topography image of the transfer-printed self-folding film. Measurement of the thickness of the film versus the number of polymer bilayers is shown in Figure 1d. The thickness of the aluminum film was precisely controlled and was kept at 100 nm. The thickness of the polymer layer, however, depends heavily on the number of bilayers deposited on the aluminum. The thickness of the polymer layer with five bilayers of PAH/PSS is 49 ± 3 nm. Increasing the number of bilayers to 10 causes the thickness to increase to 88 ± 2 nm. The polymer film composed of 15 bilayers of polyelectrolytes has a thickness of 153 ± 3 nm. After cross-linking with glutaraldehyde (15CL), the thickness decreased to 123 ± 4 nm. The change in thickness was also accompanied by a change in roughness (see Supporting Information Figure S1). The roughness (rms) was measured to be 12.16 nm for 5 bilayers, 12.70 nm for 10 bilayers, and 12.80 nm for 15 bilayers. As stated earlier, the self-folding film with 15 bilayers of polyelectrolytes is the thinnest film that showed visible response to solvent and temperature, and thus from here on discussions are focused on its characterization and response. It is expected as well that increasing the thickness of the polymer layer will cause a slower response of the bilayer film to solvent due to longer diffusion time, which is generally proportional to the square of the film thickness.[25]

Figure 2a shows the optical image of the PDMS stamp with the polymer−metal self-folding system. The success of the

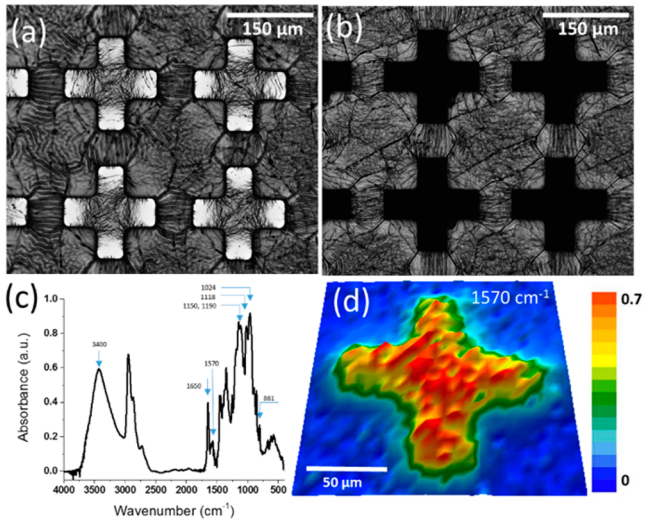

Figure 2. Optical images of the PDMS stamp before (a) and after (b) transfer-printing; black area is PDMS without self-folding film on top. (c) ATR-IR spectrum of the cross-linked polymer layer, and (d) FT-IR image (absorbance) of the transfer-printed polymer.

transfer-printing step can be seen in Figure 2b. Only the films on top of the crosses were transferred, and those at the base remained on the PDMS stamp. The success of the transfer-printing step is brought about by the stronger adhesion between the receiving substrate and the self-folding film as compared to the adhesion between the PDMS stamp and the aluminum film. Also contributing to this success is the fact that PDMS is elastic and that it can make conformal contact on any substrate over relatively large areas. Figure 2c shows the infrared spectrum of the cross-linked multilayered polymer. The peaks for the PSS are assigned as 1190 cm^{-1} for antisymmetric vibrational absorption of S═O, 1024 cm^{-1} for symmetric vibrational absorption of S═O, 1150 cm^{-1} for the in-plane skeleton vibration of benzene, 1118 cm^{-1} for the in-plane skeleton vibration of benzene, and 861 cm^{-1} for out-of-plane aromatic C−H bending.[26] On the other hand, the peaks for the PAH cross-linked by glutaraldehyde are assigned as 1650 cm^{-1} for the amide C═O stretching, 1570 cm^{-1} for the N−H (2°-amide) II band, and 3400 cm^{-1} for the N−H stretching.

The FT-IR image of the transfer-printed polymer also confirms the success of the transfer-printing technique (see Figure 2d). The FT-IR image can serve as a chemical map that contrasts regions of high organic content vs regions of low

organic content. It is therefore an optimal imaging tool to confirm if only the films on the elevated part of the PDMS stamp were transferred.[27] As can be seen on the infrared image focused at 1570 cm^{-1}, there is a high concentration of 2°-amide N−H on the cross region as evidenced by absorbance of up to 0.7. Conversely, there is no organic material on the surface outside the cross because there is very low absorbance.

The response to solvent of the transfer-printed self-folding film was observed after adding deionized water to the system. Figure 3a shows the transfer-printed self-folding films on the

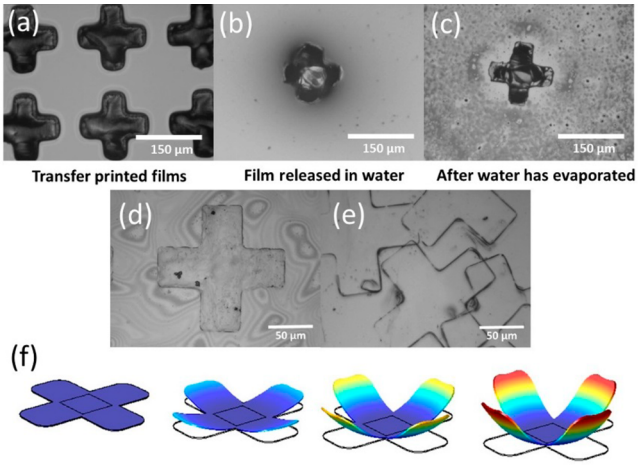

Figure 3. (a, b, c) Solvent-response of the transfer-printed self-folding film. (d) Transfer-printed 15 bilayers of PAH/PSS on PVOH, (e) released 15 bilayers of PAH/PSS film, and (f) finite-element simulation of the folding of the transfer-printed self-folding film.

PVOH sacrificial layer. After water has been added, it slowly dissolved the high molecular weight PVOH and simultaneously swelled the polymer layer. The cross-linked polymer layer is very hydrophilic due to the polar functional groups along the chain; thus it absorbs the water and, in the process, swells. The expansion of the polymer layer, however, is limited to one dimension because the aluminum film, which is covalently attached to the polymer, prevents it from expanding along the plane of the substrate. A large interfacial stress develops in-between the expanding polymer and the aluminum film because of their mismatched degrees of expansion. As the bilayer film was released from the substrate, it minimized the interfacial stress by bending or folding out of the substrate (see Figure 3b). Folding is a consequence of energy minimization and interfacial stress relaxation brought about by the stimulus. This is a common phenomenon for free-standing systems with structural heterogeneity in the direction normal to the film surface.[28] Removal of the water reverts the self-folding film back to its original 2D state (see Figure 3c). It is note-worthy that folding is only possible if there is a strong interaction between the active and the passive layer; otherwise, the expanding active layer will just be peeled off from the passive layer. This was ensured by covalently linking the aluminum film to the cross-linked polymer film by APS. The amine group of the APS is also expected to react with the glutaraldehyde cross-linker. Furthermore, the passive layer should be mechanically robust but flexible enough to facilitate the release of the interfacial stress. If the passive layer is too rigid, then the expanding active layer will just form wrinkles on the surface of the passive layer.[29]

To confirm that the bending was because of the mismatched degrees of expansion and not because of the stress in the polymer layer developed during fabrication, the polymer (without the metal layer) was transfer-printed and released in water. Figure 3d shows the transfer-printed polymer film on the PVOH sacrificial layer. Upon the dissolution of the sacrificial layer, the polymer film was released and swelled in all directions. No internal stress was developed, and thus the polymer film remained flat (see Figure 3e). To better understand the folding process due to swelling, finite-element analysis was used to model the structural changes of the bilayer system as one layer expands. As exhibited in Figure 3f, the simultaneous dissolution of the sacrificial layer and swelling of the polymer layer cause a strain on the edge of the cross. Bending starts from the edge and continues toward the center as more PVOH is dissolved.

A rectangular self-folding film (150 μm × 50 μm) was also released and was observed to curl along its length (see Figure 4a and b). This is consistent with what was observed by Li et al.

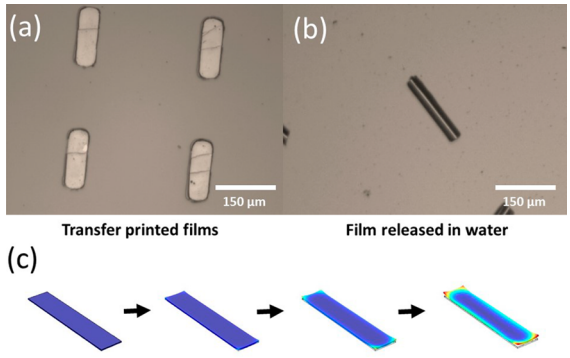

Figure 4. (a, b) Solvent-response of the rectangular self-folding film. (c) Finite-element simulation of the folding of the rectangular self-folding film.

and Schmidt et al., who experimentally showed that rectangular strips fold along the long side when the film is released from the substrate progressively.[30,31] The whole folding process is kinetically limited because of slow diffusion of water through the active layer coupled with the slow dissolution of the high molecular weight sacrificial layer. It has also been proven experimentally and with computer simulations that long-side folding is preferred for strained high aspect ratio rectangular strips (ratio of length to the width).[32] Figure 4c shows the finite-element simulation of the rectangular strip structure transformation. Consistent with what has been reported in literature, sections of the film that are closer to the edge swell first while the sections near the center do not swell. As the rectangular strip folds along the principal axis, its stiffness becomes anisotropic—it is more rigid along the length than along the width. Folding along the width is therefore not expected for this system.

The effect of the length of the rectangular strips on the radius of curvature of the resulting bent bilayer film was studied as well. Instead of using rectangular strips, rectangular strips attached to a square base to prevent it from folding along its length were used (Figure 5a). Moreover, instead of waiting for the whole film to be released, a sharp needle (50 μm wide tip) to force the rectangular strip off the sacrificial layer was utilized (see Supporting Information Figure S2). This ensures that the bending happens before the PVOH under the square base starts

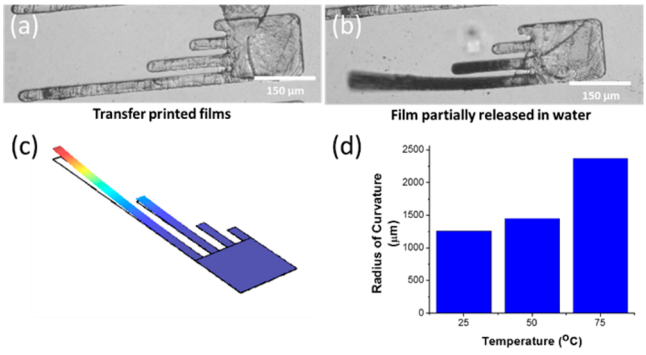

Figure 5. (a, b) Solvent-response of the rectangular strips attached to a square base. (c) Finite-element simulation of the folding of the self-folding film. (d) Change in radius of curvature of the longest strip vs temperature.

to dissolve. As can be seen in Figure 5b, the degree of bending depends on how long the rectangular strip is. The radius of curvature for the longest rectangle (L = 500 μm) is measured to be 1260 μm. The second longest barely bent out of the surface. The shortest (50 μm) and the second shortest (100 μm) seemed not to respond at all. Finite-element modeling supports the observed response of the rectangular strips. The strain that is developed on the shortest and the second shortest fingers is not sufficient to cause the surface to bend out. It is hypothesized that changing the thickness of either the metal or the polymer can alter this behavior.

Increasing the temperature of the liquid also changes the radius of curvature. This is due to the difference in the thermal expansion coefficient and the thermal conductivity of the polymer and the metal. The aluminum layer expands as the temperature is increased from 25 to 50 °C. However, its expansion is limited because of the presence of the polymer layer, which does not expand as much. The difference between the thermal expansions of the two layers caused the radius of curvature of the longest finger to increase from 1260 to 1448 μm. Further increase in temperature causes the aluminum to expand more, and, as expected, the radius of curvature increases even more. At 75 °C, the radius of curvature is increased to 2372 μm. A 50° change in temperature caused 88% increase in the radius of curvature of the longest finger. This is similar to what was reported by Ma et al. where an increase in temperature and humidity was used to actuate a bilayer film composed of thermally cross-linked PAA/PAH film and aluminum.[33]

CONCLUSION

In this study, it has been demonstrated that self-folding polymer−metal bilayer films can be effectively fabricated by using the transfer-printing technique. The transfer-printing technique proved to be a simple and an effective alternative for fabricating the bilayer film as evidenced by the optical, infrared, and AFM topography images. It is expected that the transfer-printing technique is also applicable in fabricating pure polymeric and pure inorganic self-folding systems. The fabricated self-folding film was shown to respond to solvent and to temperature. The folding was brought about by the difference in the degree of swelling and the difference in the thermal expansion coefficient and thermal conductivity of each layer.

EXPERIMENTAL SECTION

Preparation of the PDMS Stamp. The uncured PDMS solution (10 part elastomer base and 1 part curing agent, Sylgard 184, Dow Corning) was poured on the SU-8 master template. After degassing, it was cured at 60 °C for 2 h. The PDMS stamp was peeled off gently from the master template and was kept in vacuum until further use.

Fabrication of the Self-Folding Film. Very thin (100 nm thick) aluminum film was sputtered on the PDMS stamp using a Denton Vacuum DV-502A at 5 mTorr Ar, 125 W DC, producing a sputter rate of 100 Å/min. The aluminum-coated PDMS stamp was then immersed in 0.5 wt % (3-aminopropyl)trimethoxysilane (APS) (Sigma-Aldrich) for 1 h. Poly(allylamine hydrochloride) (PAH, 1 mg/mL, pH = 6.5, Sigma-Aldrich) and poly(styrenesulfonate) (PSS, 1 mg/mL in 0.1 M NaCl, Sigma-Aldrich) were alternately spin-casted on the PDMS stamp with washing in between. Cross-linking of the PAH was done by immersing the stamp in 10 wt % glutaraldehyde (Sigma-Aldrich) solution for 2 h.

Transfer Printing and Release of the Self-Folding Film. Silicon wafer substrate was cleaned by sonication in piranha solution (30% of 30% H_2O_2/70% concentrated sulfuric acid) for 20 min, Milli Q water (18.2 MΩ-cm resistivity) for 20 min and then in acetone for 20 min, and was finally cleaned by oxygen plasma for 3 min. (Caution: Piranha solution is an extremely strong oxidant and should be handled very carefully!) A thin layer of poly(vinyl alcohol) (PVOH, 3 wt %, Sigma-Aldrich) was spin-casted on the cleaned silicon wafer at 3000 rpm for 30 s. The PDMS stamp and the PVOH-coated substrate were exposed to 70 °C water vapor for 30 s. The PDMS stamp was then placed carefully on the substrate, applying slight pressure to ensure optimal contact. The PVOH was dried for at least 5 min before the stamp was slowly peeled off. The self-folding film was released by dissolving the PVOH sacrificial layer by adding water.

Finite-Element Simulation. Comsol 4.1 was used to model the self-folding system. The pure polymer rectangle was modeled using temperature as the input variable. It has been seen that the expansion of the film due to temperature increase is similar to that of the expansion due to swelling.[32] The base was fixed across the whole surface of the rectangle and was then reduced to simulate the release of the rectangle from the substrate. Crosses were simulated with arms of length 50 μm × 50 μm and a base of 50 μm × 50 μm. The base was fixed and did not allow expansion of base. It was seen that the arms would expand both laterally and would bend upward at roughly the same rate.

Instrumentation. SEM analysis was done using JEOL JSM-6510LV SEM. FT-IR imaging was conducted on Digilab FTS 7000 spectrometer, a UMA 600 microscope, and a 32 × 32 MCT IR Imaging focal plane array (MCT-FPA) image detector with an average spatial area of 176 μm × 176 μm in the reflectance mode. All atomic force microscopy images were recorded using Park AFM system Tapping Mode (Park Systems) with 45 μm × 45 μm scanner. Leica DM6000 M optical microscope, Denton Vacuum DV-502A dual-head DC sputter system nKinsten UV light box.

ASSOCIATED CONTENT

Supporting Information

Change in the measured roughness (rms) of the polymer film vs the number of layers; schematic diagram and optical image of the use of sharp needle to release the rectangular strips. This material is available free of charge via the Internet at http://pubs.acs.org.

AUTHOR INFORMATION

Corresponding Author

*E-mail: rca41@case.edu. Phone: +1 216-368-4566.

Notes

The authors declare no competing financial interest.

■ ACKNOWLEDGMENTS

We acknowledge Dr. Nicel Estillore for the preparation and synthesis of the macroinitiator. We gratefully acknowledge funding from NSF EAGER CHE-1247438, NSF-STC-0423914, and DMR-1304214 and technical support from Malvern (Viskotek), Biolin, Agilent Technologies, and Park Systems.

■ REFERENCES

(1) Stoychev, G.; Puretskiy, N.; Ionov, L. Self-Folding All-Polymer Thermoresponsive Microcapsules. *Soft Matter* **2011**, *7*, 3277−3279.
(2) Kelby, T.; Wang, M.; Huck, W. T. S. Controlled Folding of 2D Au−Polymer Brush Composites into 3D Microstructures. *Adv. Funct. Mater.* **2011**, *21*, 652−657.
(3) Liu, Y.; Boyles, J. K.; Genzer, J.; Dickey, M. Self-Folding of Polymer Sheets Using Local Light Absorption. *Soft Matter* **2012**, *8*, 1764−1769.
(4) Smela, E.; Inganäs, O.; Lundström, I. Controlled Folding of Micrometer-Size Structures. *Science* **1995**, *268*, 1735−1738.
(5) Py, C.; Reverdy, P.; Doppler, L.; Bico, J.; Roman, B.; Baroud, C. N. Capillary Origami: Spontaneous Wrapping of a Droplet with an Elastic Sheet. *Phys. Rev. Lett.* **2007**, *98*, 156103.
(6) Li, J.; Zhang, J.; Gao, W.; Huang, G.; Di, Z.; Liu, R.; Wang, J.; Mei, Y. Dry-Released Nanotubes and Nanoengines by Particle-Assisted Rolling. *Adv. Mater.* **2013**, *25*, 3715−3721.
(7) Cho, J. H.; Hu, S.; Gracias, D. H. Self-Assembly of Orthogonal Three-Axis Sensors. *Appl. Phys. Lett.* **2008**, *93*, 043505−3.
(8) Ionov, L. Soft Microorigami: Self-Folding Polymer Films. *Soft Matter* **2011**, *7*, 6786−6791.
(9) Leong, T. G.; Randall, C. L.; Benson, B. R.; Zarafshar, A. M.; Gracias, D. H. Self-Loading Lithographically Structured Microcontainers: 3D Patterned, Mobile Microwells. *Lab Chip* **2008**, *8*, 1621−1624.
(10) Leong, T.; Gu, Z.; Koh, T.; Gracias, D. H. Spatially Controlled Chemistry Using Remotely Guided Nanoliter Scale Containers. *J. Am. Chem. Soc.* **2006**, *128*, 11336−11337.
(11) He, H.; Guan, J.; Lee, J. An Oral Delivery Device Based on Self-Folding Hydrogels. *J. Controlled Release* **2006**, *110*, 339−346.
(12) Gultepe, E.; Randhawa, S.; Kadam, S.; Yamanaka, S.; Selaru, F.; Shin, E.; Kalloo, A.; Gracias, D. Biopsy with Thermally-Responsive Untethered Microtools. *Adv. Mater.* **2013**, *25*, 514−519.
(13) Timoshenko, S. Analysis of Bi-metal Thermostats. *J. Opt. Soc. Am.* **1925**, *11*, 233−233.
(14) Randhawa, J.; Keung, M.; Tyagi, P.; Gracias, D. Reversible Actuation of Microstructures by Surface-Chemical Modification of Thin-Film Bilayers. *Adv. Mater.* **2010**, *22*, 407−410.
(15) Park, J.; Hammond, P. Multilayer Transfer Printing for Polyelectrolyte Multilayer Patterning: Direct Transfer of Layer-by-Layer Assembled Micropatterned Thin Films. *Adv. Mater.* **2004**, *16*, 520−525.
(16) Carlson, A.; Bowen, A.; Huang, Y.; Nuzzo, G.; Rogers, J. Transfer Printing Techniques for Materials Assembly and Micro/Nanodevice Fabrication. *Adv. Mater.* **2012**, *24*, 39.
(17) Kim, B.; Lee, S.; Yoon, H.; Strano, M.; Shao-Horn, Y.; Hammond, P. Pattern Transfer Printing of Multiwalled Carbon Nanotube Multilayers and Application in Biosensors. *Chem. Mater.* **2010**, *22*, 4791−4797.
(18) Zhang, P.; Guan, J. Fabrication of Multilayered Microparticles by Integrating Layer-by-Layer Assembly and MicroContact Printing. *Small* **2011**, *7*, 2998−3004.
(19) Lee, N.; Lim, J.; Lee, M.; Park, S.; Kim, Y. Multilayer Transfer Printing on Microreservoir-Patterned Substrate Employing Hydrophilic Composite Mold for Selective Immobilization of Biomolecules. *Langmuir* **2006**, *22*, 7689−7694.
(20) Loo, Y.; Willett, R.; Baldwin, K.; Rogers, J. Additive, Nanoscale Patterning of Metal Films with a Stamp and a Surface Chemistry Mediated Transfer Process: Applications in Plastic Electronics. *Appl. Phys. Lett.* **2002**, *81*, 562.
(21) Perl, A.; Reinhoudt, D.; Huskens, J. Microcontact Printing: Limitations and Achievements. *Adv. Mater.* **2009**, *21*, 2257−2268.
(22) Damink, L.; Dijstra, P.; Van Luyn, M.; Van Wachem, P.; Nieuwenhuis, J.; Feijen, J. Glutaraldehyde as a Cross-Linking Agent for Collagen-Based Biomaterials. *J. Mater. Sci.: Mater. Med.* **1995**, *6*, 460−472.
(23) Tan, C. S.; Fan, A.; Chen, K. N.; Reif, R. Low-Temperature Thermal Oxide to Plasma-eEnhanced Chemical Vapor Deposition Oxide Wafer Bonding for Thin-Film Transfer Application. *Appl. Phys. Lett.* **2003**, *82*, 2649.
(24) Wang, Z.; Yuan, J.; Zhang, J.; Xing, R.; Yan, D.; Han, Y. Metal Transfer Printing and Its Application in Organic Field-Effect Transistor Fabrication. *Adv. Mater.* **2003**, *15*, 1009−1012.
(25) Tanaka, T.; Fillmore, D. J. Kinetics of Swelling of Gels. *J. Chem. Phys.* **1979**, *70*, 1214−1218.
(26) Yang, J. C.; Jablonsky, M. J.; Mays, J. W. NMR and FT-IR Studies of Sulfonated Styrene-Based Homopolymers and Copolymers. *Polymer* **2002**, *43*, 5125.
(27) Estillore, N.; Advincula, R. Stimuli-Responsive Binary Mixed Polymer Brushes and Free-Standing Films by LbL-SIP. *Langmuir* **2011**, *27*, 5997−6008.
(28) Luchnikov, V.; Ionov, L.; Stamm, M. Self-Rolled Polymer Tubes: Novel Tools for Microfluidics, Microbiology, and Drug-Delivery Systems. *Macromol. Rapid Commun.* **2011**, *32*, 1943−1952.
(29) Ionov, L. Biomimetic 3D Self-Assembling Biomicroconstructs by Spontaneous Deformation of Thin Polymer Films. *J. Mater. Chem.* **2012**, *22*, 19366.
(30) Chun, I. S.; Challa, A.; Derickson, B.; Hsia, K. J.; Li, X. Geometry Effect on the Strain-Induced Self-Rolling of Semiconductor Membranes. *Nano Lett.* **2010**, *10*, 3927.
(31) Cendula, P.; Kiravittaya, S.; Monch, I.; Schumann, J.; Schmidt, O. Directional Roll-Up of Nanomembranes Mediated by Wrinkling. *Nano Lett.* **2011**, *11*, 236.
(32) Stoychev, G.; Zakharchenko, S.; Turcaud, S.; Dunlop, J.; Ionov, L. Shape-Programmed Folding of Stimuli-Responsive Polymer Bilayers. *ACS Nano* **2012**, *6*, 3925.
(33) Ma, Y.; Sun, J. Humido- and Thermo-Responsive Free-Standing Films Mimicking the Petals of the Morning Glory Flower. *Chem. Mater.* **2009**, *21*, 898−902.